

## **Diacylglycerol lipase- $\alpha$ and - $\beta$ control neurite outgrowth in Neuro-2a cells through distinct molecular mechanisms**

Kwang-Mook Jung, Giuseppe Astarita, Dean Thongkham, and Daniele Piomelli

Department of Pharmacology (K.-M.J., G.A., D.T., D.P.) and Department of Biological Chemistry (D.P.), University of California, Irvine, Irvine, CA; Unit of Drug Discovery and Development, Italian Institute of Technology, Genova, Italy (G.A., D.P.).

**Running Title:** 2-arachidonoyl-*sn*-glycerol biosynthesis in neurite outgrowth

**Corresponding Author:** Dr. Daniele Piomelli

Department of Pharmacology, 3101 Gillespie NRF, University of California, Irvine, CA 92697-4625.

Tel: (949) 824-6180

Fax: (949) 824-6305

E-mail: [piomelli@uci.edu](mailto:piomelli@uci.edu)

Text pages: 30

Table: 0

Figures: 5

References: 42

Supplemental Table: 1

Supplemental Figures: 2

Words in Abstract: 216

Words in Introduction: 618

Words in Discussion: 1142

**Abbreviations:** ABHD,  $\alpha$ - $\beta$ -hydrolase domain; CB, cannabinoid; DAG, 1,2-diacyl-*sn*-glycerol; DGL, DAG lipase; DHPG, (S)-3,5-dihydroxyphenylglycine; DMEM, Dulbecco's Modified Eagle's Medium; EGFP, enhanced green fluorescence protein; ER, endoplasmic reticulum; ESI, electrospray ionization; FA, fatty acid; FBS, fetal bovine serum; FGF, fibroblast growth factor; GAPDH, glyceraldehyde-3-phosphate dehydrogenase; HDA, heptadecanoic acid; HDG, (1,3)-heptadecanoyl-*sn*-glycerol; LC-MS, liquid chromatography-mass spectrometry; MAG, monoacyl glycerol; mGlu, metabotropic glutamate; PCR, polymerase chain reaction; PLC, phospholipase C; RA, *all-trans*-retinoic acid; SDS-PAGE, sodium dodecylsulfate-polyacrylamide gel electrophoresis; shRNA, small-hairpin RNA; SIM, selected ion-monitoring; 2-AG, 2-arachidonoyl-*sn*-glycerol.

## Abstract

The endocannabinoid 2-arachidonoyl-*sn*-glycerol (2-AG) is produced through hydrolysis of 1,2-diacyl-*sn*-glycerol (DAG), which is catalyzed by DAG lipase (DGL). Two DGL isoforms have been molecularly cloned, but their respective roles in endocannabinoid signaling have not been fully elucidated. Here we report that DGL- $\alpha$  and DGL- $\beta$  may contribute to *all-trans*-retinoic acid (RA)-induced neurite outgrowth in neuroblastoma Neuro-2a cells through distinct mechanisms. RA-induced differentiation of Neuro-2a cells was associated with elevations of cellular 2-AG levels and DGL activity, which were accompanied by temporally separated transcription of DGL- $\alpha$  and DGL- $\beta$  mRNA. Knock-down of either DGL- $\alpha$  or DGL- $\beta$  expression attenuated neurite outgrowth, which indicates that both isoforms contribute to neuritogenesis. Immunostaining experiments showed that DGL- $\beta$  is localized to peri-nuclear lipid droplets, whereas DGL- $\alpha$  is found on plasma membranes. Following RA-induced differentiation, both DGL- $\alpha$ - and DGL- $\beta$ -GFP were distributed also in neurites, but in distinguishable patterns. Overexpression of either DGL- $\alpha$  or DGL- $\beta$  increased the number of neurite-bearing cells, but DGL- $\beta$  caused substantially larger morphological changes than DGL- $\alpha$  did. Finally, the CB<sub>1</sub> antagonist rimonabant (1  $\mu$ M) inhibited DGL- $\alpha$ -induced neuritogenesis, whereas it had no such effect on DGL- $\beta$ -induced morphological differentiation. The results indicate that RA-induced DGL expression is required for neurite outgrowth of Neuro-2a cells. The findings further suggest that DGL- $\alpha$  and - $\beta$  may regulate neurite outgrowth by engaging temporally and spatially distinct molecular pathways.

## Introduction

The endocannabinoids are a class of endogenous lipids that bind to and activate cannabinoid receptors. 2-arachidonoyl-*sn*-glycerol (2-AG) and anandamide have been identified as two major endocannabinoids and have been implicated in a variety of physiological processes (Mackie and Stella, 2006; Chevalleyre *et al.*, 2006). In the adult brain, the endocannabinoids may act as locally restricted retrograde messengers, which are produced at postsynaptic sites, travel across the synaptic cleft, and engage presynaptic CB<sub>1</sub>-type cannabinoid receptors to regulate the release of glutamate,  $\gamma$ -aminobutyric acid (GABA) and other neurotransmitters (Piomelli, 2003; Freund *et al.*, 2003; Kano *et al.*, 2009).

Evidence suggests an essential role of the endocannabinoid system during early neural development (Harkany *et al.*, 2007; Galve-Roperh *et al.*, 2006). Molecular players of the endocannabinoid system – including CB<sub>1</sub> receptors, endocannabinoid molecules and their synthesizing and degrading enzymes – have been identified from the earliest stages of embryonic development to postnatal maturation (Harkany *et al.*, 2008; Aguado *et al.*, 2005; Aguado *et al.*, 2006; Berghuis *et al.*, 2005). CB<sub>1</sub> receptors are enriched in axonal growth cones of the pyramidal neurons and GABAergic interneurons of the developing rodent brain, and neurons lacking CB<sub>1</sub> receptors displayed impaired axonal path finding and target selection (Berghuis *et al.*, 2007; Mulder *et al.*, 2008). These data identify endocannabinoids as axon guidance cues and implicate CB signaling in the regulation of synaptogenesis and target selection *in vivo*. In cultured cells, activation of CB<sub>1</sub> receptors causes neurite outgrowth by regulating the proteasomal degradation of Rap1GAPII and activating Rap1 and Src-Stat3 signaling (Jordan *et al.*, 2005; He *et al.*, 2005; Bromberg *et al.*, 2008). Moreover, inhibition of 2-AG synthesis attenuates fibroblast growth factor (FGF)-induced neurite outgrowth in primary cerebellar neurons (Williams *et al.*, 2003; Bisogno *et al.*, 2003), suggesting that 2-AG might be specifically involved in the activation of CB<sub>1</sub> receptor-dependent neurite outgrowth.

2-AG is produced from the sequential hydrolysis of membrane phosphatidylinositol-4,5-bisphosphate into 1,2-diacyl-*sn*-glycerol (DAG), which is catalyzed by phospholipase C- $\beta$  (PLC- $\beta$ ), and then of DAG into 2-AG, which is catalyzed by DAG lipase (DGL) (Stella *et al.*, 1997; Piomelli, 2003). 2-AG is further cleaved by monoacylglycerol lipase or  $\alpha$ - $\beta$ -hydrolase domain (ABHD)-6 (Piomelli, 2004; Blankman *et al.*, 2007), to be deactivated. Two mammalian isoforms of DGL have been cloned: DGL- $\alpha$  and DGL- $\beta$  (Bisogno *et al.*, 2003). DGL- $\alpha$  is expressed in the hippocampus, striatum, ventral tegmental area and cerebellum of adult mouse brain (Katona *et al.*, 2006; Yoshida *et al.*, 2006; Uchigashima *et al.*, 2007; Mátyás *et al.*, 2008), where it is thought to initiate 2-AG-mediated signaling at excitatory synapses (Katona and Freund, 2008; Tanimura *et al.*, 2010; Gao *et al.*, 2010). By contrast, the functional roles of DGL- $\beta$  in the adult brain are largely unknown. Time-dependent expression for both DGL- $\alpha$  and DGL- $\beta$  has been observed in neurons during development at developing axonal tracts (Watson *et al.*, 2008; Berghuis *et al.*, 2007; Buckley *et al.*, 1998; Bisogno *et al.*, 2003), however, the contribution of DGL and 2-AG signaling to the control of neurite outgrowth has not been investigated on the molecular level.

In the present study, we asked whether transcriptional control of DGL expression and subsequent activation of 2-AG-mediated signaling contribute to *all-trans*-retinoic acid (RA)-induced neuronal differentiation in neuroblastoma Neuro-2a cells. We found that RA stimulates expression of both DGL- $\alpha$  and DGL- $\beta$ , and elevates 2-AG levels, which are required for neurite outgrowth in Neuro-2a cells. Both  $\alpha$ - and  $\beta$ -isoform of DGL, upon exogenous expression in Neuro-2a cells, increased 2-AG levels and triggered neurite outgrowth. Unexpectedly, we found segregative signaling characteristics between the two DGL isoforms, e.g., distinguishable subcellular localization and differential sensitivity to CB<sub>1</sub> receptor blockade. Our findings suggest that transcriptional regulation of DGL- $\alpha$  and DGL- $\beta$  contributes to RA-induced neurite outgrowth through temporally and spatially distinct cellular signaling pathways.

## Materials and Methods

### Chemicals

Hexadecanoic acid, heptadecanoic acid, octadecanoic acid,  $\Delta^9$  octadecenoic (oleic) acid,  $\Delta^{9,12}$  octadecadienoic acid,  $\Delta^{9,12,15}$  octadecatrienoic acid,  $\Delta^{8,11,14}$  eicosatrienoic acid, eicosatetraenoic acid, eicosapentaenoic acid, docosahexaenoic acid, (1,3)-palmitoyl-*sn*-glycerol, (1,3)-heptadecanoyl-*sn*-glycerol, (1,3)-stearoyl-*sn*-glycerol, (1,3)-linolenoyl-*sn*-glycerol, (1,3)-eicosatrienoyl-*sn*-glycerol, (1,3)-docosahexaenoyl-*sn*-glycerol were from Nu-Chek Prep (Elysian, MN). 2-AG, 2-linoleoyl-*sn*-glycerol, noladin ether, JZL184 and WWL70 were from Cayman Chemicals (Ann Arbor, MI), and 2-oleoyl-*sn*-glycerol and carbachol from Sigma-Aldrich (St. Louis, MO). (S)-3,5-dihydroxyphenylglycine (DHPG) was obtained from Tocris (Ellisville, MO). Rimonabant (SR141716A) was from RTI International (Research Triangle Park, NC). Solvents were purchased from Burdick and Jackson's (Muskegon, MI).

### Plasmids

We amplified the full-length coding sequence of DGL- $\beta$  by polymerase chain reaction (PCR), using first-strand mouse brain cDNAs as a template. High Fidelity PCR Master (Roche, Indianapolis, IN) was used for the amplification, following the manufacturer's protocol. The primers were 5'-DGL- $\beta$  (5'-GTGGGAGGTGCGCCATGCC-3') and 3'-DGL- $\beta$  (5'-CGGTACACTTGAGCCGCTTGCC-3'). The PCR product was subcloned into a pEF-V5-His vector by TOPO cloning (Invitrogen, Carlsbad, CA). Mouse DGL- $\alpha$  and DGL- $\alpha$ -pEGFP constructs were prepared as previously described (Jung *et al.*, 2007). A construct encoding an enhanced green fluorescence protein (EGFP)-fusion protein to the C-terminal of DGL- $\beta$  was generated in a pEGFP-N2 vector (Clontech, Mountain View, CA) using a Sal I site. All constructs obtained through PCR amplifications were verified by DNA sequencing. Cloning and screening of small-hairpin RNA (shRNA) constructs targeting mouse DGL- $\beta$  were performed as

previously described for DGL- $\alpha$  shRNA (Jung *et al.*, 2007). Briefly, we designed the shRNA constructs that contained both a cytomegalovirus promoter-driven GFP and a U6 promoter-driven shRNA expression system using BLOCK-iT RNAi Designer (<https://rnaidesigner.invitrogen.com/rnai-express/>), and synthesized the corresponding oligonucleotides. Oligonucleotides used for DGL- $\alpha$  has been previously described (Jung *et al.*, 2007). The oligonucleotides for DGL- $\beta$ , which was selected after screening six independent shRNA sequences as described below, was 5'-CACCGCAGTACAGGGATTTTCATTCACGAATGAATGAAATCCCTGTACTGC-3' (top) and 5'-AAAAGCAGTACAGGGATTTTCATTCATTCGTGAATGAAATCCCTGTACTGC-3' (bottom). Sense and antisense oligonucleotides were annealed and ligated into pENTR entry vector (Invitrogen) to generate U6 promoter-shRNA-Pol III terminator cassette. RNAi silencing was tested from six independent constructs by quantitative PCR and western blotting. The selected shRNA expression cassette was amplified by PCR using M13F and M13R primers containing a MluI overhang at both 5' and 3' ends. The PCR product was ligated into an adeno-associated virus vector (pAAV-hrGFP; Stratagene) using MluI sites.

### **Cell cultures and western blot analyses**

We transfected Neuro-2a cells (American Type Culture Collection, Manassas, VA) using Superfect reagent (Qiagen, Valencia, CA) as recommended by the manufacturer, and incubated them until harvest at 37°C with 5% CO<sub>2</sub> in Dulbecco's Modified Eagle's Medium (DMEM) (Gibco-Invitrogen, Carlsbad, CA) supplemented with 10% fetal bovine serum (FBS) and antibiotics (Gibco-Invitrogen). Stable DGL expressing cell lines were generated by transfecting Neuro-2a cells in a 100-mm dish with 10  $\mu$ g of control pEF6, DGL- $\alpha$ -V5-pEF6 or DGL- $\beta$ -V5-pEF6. Individual blasticidin-resistant colonies were isolated 14 days after transfection and screened for DGL expression by western blotting using a monoclonal anti-V5 antibody

(Invitrogen). Stable cell lines were maintained in DMEM with 10% FBS and penicillin/streptomycin in the presence of 10 µg/ml blasticidin (Invitrogen). For protein analyses, we prepared lysates in a buffer containing Tris-HCl (10 mM, pH 7.4), NaCl (150 mM), Triton X-100 (1%), Nonidet P-40 (0.25%), EDTA (2 mM) supplemented with a mixture of protease inhibitors (Roche). Lysates were centrifuged at 14,000 x g for 10 min and protein concentrations from the supernatants were measured using BCA protein assay (Pierce, Rockford, IL). Proteins (20 µg) were separated by 4-20% sodium dodecylsulfate-polyacrylamide gel electrophoresis (SDS-PAGE), transferred to PVDF membranes, and subjected to western blotting. We used monoclonal anti-V5 (1:5,000, Invitrogen), polyclonal anti-DGL-β (1:3,000)(Jung *et al.*, 2005) or monoclonal anti-Actin (1:10,000, Calbiochem, San Diego, CA) as primary antibodies.

### Lipid analyses

Lipid analyses were conducted by liquid chromatography-mass spectrometry (LC-MS), as previously described (Jung *et al.*, 2007; Astarita *et al.*, 2008; Astarita *et al.*, 2009). Briefly, cells were rinsed with ice-cold phosphate-buffered saline and scraped into 1 ml of methanol/water (1:1, vol:vol). Protein concentrations were measured with a BCA protein assay kit (Pierce). Lipids were extracted into a chloroform/methanol mixture (2:1, vol:vol; 1.5 ml) containing (1,3)-heptadecanoyl-*sn*-glycerol (HDG) and heptadecanoic acid (HDA) as internal standards (100 pmol/sample). Organic phases were collected, dried under N<sub>2</sub> and dissolved in methanol/chloroform (3:1, vol:vol) for analyses.

*Monoacylglycerols (MAG)* – We used an Agilent 1100-LC system coupled to a 1946D-MS detector equipped with an electrospray ionization (ESI) interface (Agilent Technologies, Inc., Palo Alto, CA). MAGs were separated on a reversed-phase XDB Eclipse C18 column (50x4.6 mm i.d., 1.8 µm, Zorbax, Agilent Technologies). They were eluted with a gradient of methanol in water (from 85% to 90% methanol in 2.0 min and 90% to 100% in 3.0 min) at a flow rate of 1.5



ml/min. Column temperature was kept at 40°C. MS detection was in the positive ionization mode, capillary voltage was set at 3 kV and fragmentor voltage was 120 V. N<sub>2</sub> was used as drying gas at a flow rate of 13 l/min and a temperature of 350°C. Nebulizer pressure was set at 60 PSI. Commercial MAGs were used as reference standards. For quantification purposes, we monitored the Na<sup>+</sup> adducts of the molecular ions [M+Na]<sup>+</sup> in the selected ion-monitoring (SIM) mode, using HDG (mass-to-charge ratio,  $m/z = 367$ ) as an internal standard. *Non-esterified fatty acids (FA)* – We used a reversed-phase XDB Eclipse C18 column (50x4.6 mm i.d., 1.8 µm, Zorbax, Agilent Technologies) eluted with a linear gradient from 90% to 100% of A in B for 2.5 min at a flow rate of 1.5 ml/min with column temperature at 40°C. Mobile phase A consisted of methanol containing 0.25% acetic acid and 5 mM ammonium acetate; mobile phase B consisted of water containing 0.25% acetic acid and 5 mM ammonium acetate. ESI was in the negative mode, capillary voltage was set at 4 kV and fragmentor voltage was 100 V. N<sub>2</sub> was used as drying gas at a flow rate of 13 l/min and a temperature of 350°C. Nebulizer pressure was set at 60 PSI. We used commercially available fatty acids as reference standards, monitoring deprotonated molecular ions [M-H]<sup>-</sup> in the SIM mode. HDA ( $m/z = 269$ ) was used as an internal standard.

### **Fluorescence immunostaining and neurite outgrowth assay**

We cultured Neuro-2a cells on Labtek chamber slides (Nunc, Roskilde, Denmark), transfected, fixed and immunostained them as described (Jung *et al.*, 2005). Monoclonal anti-V5 (1:2000, Invitrogen), polyclonal anti-V5 (1:500, Covance, Berkeley, CA) and monoclonal anti-β-Tubulin (1:1000, Sigma-Aldrich, St. Louis, MO) were used as primary antibodies. Alexa 488- or Alexa 546-labeled secondary antibodies (1:1000, Molecular Probes, Eugene, OR) were used for detection. BODIPY 493/503 (1:1000, Molecular Probes) was used to stain lipid droplets in Neuro-2a cells treated with 400 µM oleate for 18 hours, and DAPI-containing media (Vector

Laboratories, Burlingame, CA) was used for nucleus staining and mounting. We captured the images using an Eclipse E600 fluorescence microscope (Nikon, Japan) equipped with a digital camera (Diagnostic Instruments, Sterling Heights, MI). For neurite outgrowth assay, images from random fields of stained cells were manually analyzed in a blind fashion. We considered neurite-bearing cells for those displaying more than one process which is at least twice the length of the cell body. For each culture condition, we scored three regions from the slide containing more than 100 cells. Neurite lengths were measured only from the neurite-bearing cells.

### **mRNA quantification**

We measured mRNA levels using a quantitative real-time PCR method. We extracted RNA from cultured cells using a TRIzol (Invitrogen)/RNeasy (Qiagen) hybrid method and synthesized first-strand complementary DNA from 2 µg of total RNA. Reverse transcription was carried out using Superscript II RNase H reverse transcriptase (Invitrogen) and oligo(dT)12-18 primers, for 50 min at 42°C. Quantitative PCR was conducted using Mx3000P system (Stratagene). DGL mRNA levels were normalized using glyceraldehyde-3-phosphate dehydrogenase (GAPDH) as an internal standard. The primer/probe sets were as follows: for mouse DGL- $\alpha$  (GI: 54312093), forward, 5'-CCAGGCCTTTGGGCG-3'; reverse, 5'-GCCTACCACAATCAGGCCAT-3'; TaqMan probe, 5'-ACCTGGGCCGTGGAACCAAACA-3' and for mouse CB<sub>1</sub> receptor, forward, 5'-CACAAGCACGCCAATAACACA-3'; reverse, 5'-ACAGTGCTCTTGATGCAGCTTTC-3'; TaqMan probe, 5'-CCAGCATGCACAGGGCCGC-3' (TIB Molbiol, Adelphia, NJ). We used Taqman gene expression assays for mouse DGL- $\beta$  (Mm00523381\_m1), MGL (Mm00449274\_m1) and ABHD6 (Mm00481199\_m1) (Applied Biosystems, Foster City, CA).

### ***In vitro* DGL activity assay**

We harvested cells in 50 mM Tris-HCl (pH 7.0, 1 ml/dish) and homogenized them by passing through a 23-gauge needle for 20 times. The homogenates were centrifuged at 800 x *g* for 5 min at 4°C, and the resulting supernatants were used for the assays. DGL activity was measured at 37°C for 30 min in 50 mM Tris-HCl, pH 7.0, containing 0.1% Triton X-100, 0.1 mg of cellular protein and substrate diheptadecanoylglycerol (50 μM). Reactions were stopped by adding chloroform-methanol (1:1, vol:vol) containing [<sup>2</sup>H<sub>8</sub>]-2-AG (100 pmol/sample). Lipids were extracted and monoheptadecanoylglycerol was quantified as [M+Na]<sup>+</sup> (*m/z* = 367) by LC-MS using [<sup>2</sup>H<sub>8</sub>]-2-AG (*m/z* = 409) as an internal standard.

### **Statistical analyses**

Results are expressed as means ± SEM. Analyses were conducted with GraphPad Prism v.4.0 (GraphPad Software, San Diego, CA) and differences were considered significant if *P* < 0.05 by two-tailed Student's *t*-test.

## Results

### **RA-induced differentiation of Neuro-2a cells is associated with temporally distinct changes in DGL- $\alpha$ and DGL- $\beta$ expression**

Treatment of Neuro-2a cells with RA (20  $\mu$ M) resulted in extensive formation and elongation of neurite-like processes (Fig. 1A and 1B). Carbachol, a pan-agonist for muscarinic acetylcholine receptors, modestly but significantly increased neurite outgrowth after 48 hours of treatment, whereas DHPG (100  $\mu$ M), a group I mGlu receptor agonist, had no such effect (Fig. 1B). The RA-induced neurite outgrowth was partially, but significantly attenuated by pre-treatment with the selective CB<sub>1</sub> receptor antagonist rimonabant (1  $\mu$ M, 24 hours) (Fig. 1C), without affecting cell viability (Supplementary Fig. S1), suggesting that an endocannabinoid signal might be involved in RA-induced neurite outgrowth. To test this possibility, we quantified two main endocannabinoids, 2-AG and anandamide, in cell cultures treated with RA. Cellular levels of 2-AG, but not anandamide, were significantly elevated in RA-treated cells, compared to vehicle-treated controls (Fig. 1D). Consistent with this result, we found that RA increased cellular DGL activity, measured in cell homogenates (Fig. 1E).

We further examined whether RA affects the expression of DGL- $\alpha$  and DGL- $\beta$ . We found that RA caused a time-dependent increase in DGL- $\alpha$  mRNA, which was statistically significant starting from day 1 of treatment (Fig. 2A). We also observed an increase in DGL- $\beta$  mRNA, which was quantitatively smaller and temporally delayed relative to DGL- $\alpha$  (Fig. 2B). Additionally, significant increases in CB<sub>1</sub> receptor and ABHD6 mRNA were observed after 3 days of RA treatments, while MGL mRNA was not detectable in Neuro-2a cells (Fig. 2C). Similar changes in mRNA levels, which were accompanied by morphological differentiations, were also observed in SH-SY5Y human neuroblastoma cells treated with RA for 7 days; DGL- $\alpha$  (control,  $2.25 \pm 0.15$ ; RA,  $6.65 \pm 0.67$ ,  $P=0.003$ ),

DGL- $\beta$  (control,  $1.33 \pm 0.10$ ; RA,  $4.497 \pm 0.93$ ,  $P=0.027$ ) and CB $_1$  receptor (control,  $0.014 \pm 0.002$ ; RA,  $0.91 \pm 0.07$ ,  $P<0.001$ ) (mRNA ratio to GAPDH  $\times 1,000$ ,  $n=3$  each).

Next, we used RNA interference to test whether DGL expression is required for RA-induced neuronal differentiation. The efficiency and selectivity of shRNA-induced knock-down of DGL isoforms were confirmed by western blot, immunostaining and quantitative PCR methods (Jung *et al.*, 2007; data not shown). We found that cells transfected with either DGL- $\alpha$ - or DGL- $\beta$ -silencing shRNA, compared to control non-targeting shRNA, displayed significantly less neurite outgrowth after 48 hours of RA treatment (Fig. 2D). Co-transfection with DGL- $\alpha$ - and DGL- $\beta$ -silencing shRNAs resulted in a marked inhibition of neurite outgrowth, which was significantly greater than that produced by DGL- $\beta$ -shRNA alone.

We further asked whether 2-AG is a mediator for neurite outgrowth signal. We observed that treatment with a stable analogue of 2-AG, noladin ether (10  $\mu$ M, 48 hours), resulted in increased neuritogenesis of Neuro-2a cells (Fig. 2E). In addition, inhibition of 2-AG hydrolysis using the ABHD6 inhibitor WWL70 (10  $\mu$ M) caused a modest but significant increase in neurite outgrowth. Consistent with the lack of MGL expression in Neuro-2a cells (see above), the MGL inhibitor JZL184 (1  $\mu$ M) had no effect on neuritogenesis (Fig. 2E).

**DGL- $\beta$  localizes to perinuclear lipid droplets** The temporal difference between RA-induced expression of DGL- $\alpha$  and DGL- $\beta$  suggests a segregation in cellular function of these two DGL isoforms. We and others have previously reported that DGL- $\alpha$  localizes to the plasma membrane of neuronal cells (Jung *et al.*, 2007; Katona *et al.*, 2006). To determine the subcellular localization of DGL- $\beta$ , we constructed and expressed a C-terminal GFP-fused DGL- $\beta$  in Neuro-2a cells. DGL- $\beta$ -GFP fluorescence was primarily concentrated in an intracellular peri-nuclear compartment (Fig. 3A), unlike DGL- $\alpha$ -GFP

or control GFP (Jung *et al.*, 2007). Similar results were obtained when the proteins were expressed in HEK-293 cells (Fig. 3B). In double-fluorescence staining experiments, DGL- $\beta$ -GFP signal did not overlap with that of either nuclear or endoplasmic reticulum (ER) marker proteins (data not shown). Instead, DGL- $\beta$  immunofluorescence (Fig. 3C, Anti-V5), but not DGL- $\alpha$  immunofluorescence, overlapped with lipid droplet staining (Fig. 2C, BODIPY) in transiently transfected Neuro-2a cells. Alterations in the size and distribution of lipid droplets were also noticeable in DGL- $\beta$ -overexpressing cells (Fig. 3C). In cells differentiated with RA, DGL- $\alpha$ -GFP and DGL- $\beta$ -GFP were localized to neurite-like structures, in addition to the plasma membrane and perinuclear lipid droplets distributions, respectively (Fig. 3D). In neurites, expression of DGL- $\alpha$ -GFP was highly concentrated in large clusters at membranes whereas partially punctuated signals from DGL- $\beta$ -GFP were dispersed throughout the neurites (Fig. 3D).

#### **Overexpression of DGL- $\alpha$ or DGL- $\beta$ promotes constitutive neurite outgrowth through CB and non-CB mechanisms**

Next, we investigated the effect of DGL overexpression on cellular 2-AG biosynthesis and neurite outgrowth. Transient overexpression of DGL- $\beta$ -V5 (Supplementary Fig. S2A) caused a significant increase in cellular 2-AG levels, compared to control, vector-transfected cells (Supplementary Fig. S2B) and caused lipidomic changes that are comparable to those observed after DGL- $\alpha$  overexpression (Supplementary Table 1) (Jung *et al.*, 2007). We found that transient overexpression of either DGL- $\alpha$  or DGL- $\beta$  results in significant increases of neurite-bearing cells (Fig. 4A and Supplementary Fig. S2C). It is notable that DGL- $\beta$  expression caused neurite formation in a significantly higher number of cells compared to DGL- $\alpha$  expression (Fig. 4A). We further established Neuro-2a cell lines that stably express DGL- $\alpha$ -V5 ( $\alpha$ 18) or DGL- $\beta$ -V5 ( $\beta$ 14), as described in Materials and Methods.

Microscopic observations revealed constitutive morphological changes in  $\beta$ 14 cells, which included extended neurite outgrowth and filopodia-like protrusions (Fig. 4B: top, light microscopic images; bottom,  $\beta$ -tubulin-immunofluorescence).  $\alpha$ 18 cells also displayed morphological changes, albeit to a lesser extent than did  $\beta$ 14 cells (Fig. 4B). The number of neurite-bearing cells was significantly higher in both  $\alpha$ 18 and  $\beta$ 14 cells, compared with stable vector-transfected P7 cells (Fig. 4C). The mean length of neurite was significantly higher in  $\beta$ 14 cells, compared to P7 cells, but not in  $\alpha$ 18 cells (Fig. 4D). In contrast, average number of neurites from individual neurite-bearing cells showed no differences (data not shown). Finally, we tested whether neurite outgrowth triggered by DGL overexpression is mediated by CB<sub>1</sub> receptors. The  $\alpha$ 18 and  $\beta$ 14 cells, along with control P7 cells, were treated with rimonabant (1  $\mu$ M) for 24 hours. Strikingly, whereas DGL- $\alpha$ -induced neurite outgrowth was almost completely inhibited by rimonabant, CB<sub>1</sub> blockade did not affect DGL- $\beta$ -induced neurite outgrowth (Fig. 5). The results indicate that the neuritogenic effect of DGL- $\alpha$  expression is mediated through CB<sub>1</sub> receptor activation, presumably via 2-AG, whereas DGL- $\beta$  expression operates through a CB<sub>1</sub>-independent pathway.

## **Discussion**

In the present study, we investigated the role of DGL isoforms, DGL- $\alpha$  and DGL- $\beta$ , in the control of neurite outgrowth of Neuro-2a cells. Our results indicate that both DGL- $\alpha$  and DGL- $\beta$  contribute to RA-induced neuritogenesis, but through two distinct mechanisms: DGL- $\alpha$  by initiating 2-AG-mediated endocannabinoid signaling at plasma membranes, and DGL- $\beta$  by engaging an as-yet-uncharacterized molecular pathway possibly through intracellular lipid droplets.

We found that RA elevates cellular 2-AG levels and DGL activity in Neuro-2a cells. These increases were due, at least in part, to a transcriptional up-regulation of DGL- $\alpha$  and DGL- $\beta$ , which occurred, however, within distinguishable time frames, DGL- $\alpha$  expression being more rapid and pronounced than DGL- $\beta$ 's. These molecular events were associated with increased neuronal differentiation, as previously observed in neuroblastoma cells *in vitro*, in response to RA treatment (Clagett-Dame *et al.*, 2006; Dehmelt *et al.*, 2003; Wu *et al.*, 1995). On the other hand, agonists for either mGlu5 receptor or muscarinic acetylcholine receptors, which are both known to increase 2-AG levels in the adult brain, caused little or no neurite outgrowth compared to RA. This result could be due to differences between developing and mature neurons. This idea corroborated by the fact that the localization of DGL- $\alpha$  changes dramatically during development (Berghuis *et al.*, 2007; Watson *et al.*, 2008; Bisogno *et al.*, 2003). We found that, importantly, RNAi-induced silencing of either DGL- $\alpha$  or DGL- $\beta$  attenuates neurite outgrowth, suggesting that both DGL isoforms may contribute to RA-induced differentiation. In addition, knock-down of both DGL- $\alpha$  and DGL- $\beta$  resulted in an additive inhibitory effect on neuritogenesis. A significant difference was found between silencing DGL- $\alpha$  alone or in combination with DGL- $\beta$ . This suggests that DGL- $\alpha$  may exert its effects, at least in part independently of DGL- $\beta$ .



Our immunostaining studies of undifferentiated Neuro-2a cells suggest that DGL- $\beta$  is localized to lipid droplets, whereas DGL- $\alpha$  is mainly found at plasma membranes (Katona *et al.*, 2006; Jung *et al.*, 2007). DGL- $\alpha$  has been previously identified at the plasma membrane of glutamatergic synapses and its contribution to metabotropic glutamate (mGlu) receptor-dependent plasticity has been extensively studied (Maejima *et al.*, 2001; Varma *et al.*, 2001; Katona *et al.*, 2006; Jung *et al.*, 2007). Electrophysiological or pharmacological stimulation of mGlu5 receptors produces 2-AG, mainly from the sequential hydrolysis of phosphatidylinositol-4,5-bisphosphate by PLC- $\beta$  and DGL- $\alpha$  (Stella *et al.*, 1997; Jung *et al.*, 2005), which then acts on presynaptic CB<sub>1</sub> receptors to regulate neurotransmitter release. Inhibition of phosphatidylinositol-specific PLC activities abrogated the receptor-dependent upregulation of 2-AG biosynthesis, indicating that there is a preference for utilizing phosphoinositides, among various species of membrane phospholipids, as the precursor of 2-AG. This might be, at least in part, due to the assembly of the receptor with signal transducing enzymes, PLC- $\beta$  and DGL- $\alpha$ , in a macromolecular protein complex which is mediated by direct interactions with scaffolding proteins such as Homer and Shank (Hwang *et al.*, 2005; Katona *et al.*, 2006; Jung *et al.*, 2007). Recent work with genetically modified mice has confirmed such a role of DGL- $\alpha$  in synaptic regulations (Tanimura *et al.*, 2010; Gao *et al.*, 2010). By contrast, the functions of DGL- $\beta$  are still largely unknown. The localization of this DGL isoform in lipid droplets, which are emerging as important intracellular organelles involved in lipid homeostasis (Digel *et al.*, 2010), suggests that DGL- $\beta$  may be involved in regulating membrane dynamics during neuritogenesis. This hypothesis deserves further investigation.

We found that, in Neuro-2a cells differentiated by RA, both DGL- $\alpha$  and DGL- $\beta$  localize to neurite structures in addition to their main site of distribution sites in non-differentiated

cells. This is in accordance with a previous report indicating that most, if not all, developing axonal tracks co-express both DGL isoforms (Bisogno *et al.*, 2003). Moreover, our results indicate that the distributions of DGL isoforms in neurites are distinguishable. Fluorescence signals from DGL- $\alpha$ -GFP were highly concentrated in large clusters at membranes, whereas DGL- $\beta$ -GFP were dispersed throughout the neurites displaying partially punctuated signals. Distinctive axonal distributions of the two DGL isoforms had been found in embryonic pyramidal cells, where DGL- $\alpha$  is concentrated in axonal varicosities, whereas DGL- $\beta$  is distributed uniformly along axons. Additionally, in axonal growth cones, DGL- $\alpha$  is targeted to filopodia, whereas DGL- $\beta$  is concentrated in the axon stem with a clear demarcation from the growth cones (Mulder *et al.*, 2008). The distributions of both DGL isoforms in elongating neurites, in a distinguishable manner, support the idea that both DGL- $\alpha$  and DGL- $\beta$  contribute to RA-induced neuritogenesis through distinct mechanisms.

Transient or stable overexpression of either DGL- $\alpha$  or DGL- $\beta$  induces constitutive morphological changes in Neuro-2a cells. We found that DGL- $\beta$  expression is more effective than DGL- $\alpha$  at inducing neurite outgrowth, which was even more striking after normalization with efficiency of DGL protein expression (data not shown). Importantly, DGL- $\beta$  expression promotes neurite elongation, whereas DGL- $\alpha$  does not. The results indicate that functional expression of either DGL isoform, which is expected to increase 2-AG levels in two different subcellular locations, is sufficient to initiate neurite outgrowth. On the other hand, our targeted lipidomic analyses revealed that DGL- $\alpha$  and DGL- $\beta$ , when overexpressed in Neuro-2a cells, cause similar lipidomic changes in cells (Jung *et al.*, 2007). DGL- $\beta$  expression increased levels of 2-AG and other unsaturated fatty acid-containing MAGs as well as unsaturated free fatty acids that result from increased 2-acylglycerol hydrolysis. Consistent with these findings, it has been reported

that two DGL isoforms display similar biochemical properties *in vitro* (Bisogno *et al.*, 2003). In addition, a bioinformatics comparison between the two DGL isoforms indicates that DGL- $\beta$  has extensive structural and sequence homology with DGL- $\alpha$ , e.g. four transmembrane-spanning domains, a lipase-3 motif and a serine lipase motif. But DGL- $\beta$  lacks a large C-terminal fragment found in DGL- $\alpha$ . The C-terminal “tail” domain, which is followed by the catalytic motif in DGL- $\alpha$  (Bisogno *et al.*, 2003), contains a few hypothetical post-translational modification sites, as well as the Homer binding motif, which is responsible for its association with mGlu receptor-containing multiprotein complex at plasma membranes (Jung *et al.*, 2007). These results indicate that the differential control of expression, subcellular positioning and structural divergence between DGL- $\alpha$  and DGL- $\beta$ , rather than differences in enzymatic characteristics, lead to the observed distinctions in physiological function. The CB<sub>1</sub> antagonist rimonabant significantly inhibited DGL- $\alpha$ -induced neurite outgrowth, but failed to prevent DGL- $\beta$ -induced neuritogenesis. An economical interpretation of these results is that DGL- $\beta$  expression targets an unknown intracellular pathway that is independent from 2-AG signaling at the CB<sub>1</sub> receptors.

Although our results support the role of DGL in axonal growth and guidance, there are, at least apparently, conflicting observations during differentiation of neural stem cell line Cor-1 (Walker *et al.*, 2010). These discrepancies suggest that 2-AG signaling might be linked to neural differentiation in a cell- and developmental stage-dependent manner.

In conclusion, our study indicates that RA induces the functional expression of DGL, which is required for neurite outgrowth of Neuro-2a cells, and that DGL- $\alpha$  and DGL- $\beta$  may engage differential cellular mechanisms to regulate neuronal differentiation.

## **Acknowledgements**

The contributions of the Agilent Technologies/University of California, Irvine Analytical Discovery Facility, Center for Drug Discovery is gratefully acknowledged.

## **Authorship Contributions**

Participated in research design: Jung, Piomelli

Conducted experiments: Jung, Astarita, Thongkham

Performed data analysis: Jung, Astarita, Thongkham

Wrote the manuscript: Jung, Astarita, Piomelli

## References

- Aguado T., Monory K., Palazuelos J., Stella N., Cravatt B., Lutz B., Marsicano G., Kokaia Z., Guzmán M. and Galve-Roperh I. (2005) The endocannabinoid system drives neural progenitor proliferation. *FASEB J.* **19**, 1704-1706.
- Aguado T., Palazuelos J., Monory K., Stella N., Cravatt B., Lutz B., Marsicano G., Kokaia Z., Guzmán M. and Galve-Roperh I. (2006) The endocannabinoid system promotes astroglial differentiation by acting on neural progenitor cells. *J. Neurosci.* **26**, 1551-1561.
- Astarita G., Ahmed F. and Piomelli D. (2008) Identification of biosynthetic precursors for the endocannabinoid anandamide in the rat brain. *J. Lipid Res.* **49**, 48-57.
- Astarita G. and Piomelli D. (2009) Lipidomic analysis of endocannabinoid metabolism in biological samples. *J. Chromatogr. B. Analyt. Technol. Biomed. Life Sci.* **877**, 2755-2767.
- Berghuis P., Dobszay M.B., Wang X., Spano S., Ledda F., Sousa K.M., Schulte G., Ernfors P., Mackie K., Paratcha G., Hurd Y.L. and Harkany T. (2005) Endocannabinoids regulate interneuron migration and morphogenesis by transactivating the TrkB receptor. *Proc. Natl. Acad. Sci. USA* **102**, 19115-19120.
- Berghuis P., Rajnicek A.M., Morozov Y.M., Ross R.A., Mulder J., Urbán G.M., Monory K., Marsicano G., Matteoli M., Canty A., Irving A.J., Katona I., Yanagawa Y., Rakic P., Lutz B., Mackie K. and Harkany T. (2007) Hardwiring the brain: endocannabinoids shape neuronal connectivity. *Science* **316**, 1212-1216.
- Bisogno T., Howell F., Williams G., Minassi A., Cascio M.G., Ligresti A., Matias I., Schiano-Moriello A., Paul P., Williams E.J., Gangadharan U., Hobbs C., Di Marzo V. and Doherty P. (2003) Cloning of the first sn1-DAG lipases points to the spatial and temporal regulation of endocannabinoid signaling in the brain. *J. Cell Biol.* **163**, 463-468.

- Blankman J.L., Simon G.M. and Cravatt B.F. (2007) A comprehensive profile of brain enzymes that hydrolyze the endocannabinoid 2-arachidonoylglycerol. *Chem. Biol.* **14**, 1347-1356.
- Bromberg K.D., Iyengar R. and He J.C. (2008) Regulation of neurite outgrowth by G(i/o) signaling pathways. *Front. Biosci.* **13**, 4544-4557.
- Buckley N.E., Hansson S., Harta G. and Mezey E. (1998) Expression of the CB1 and CB2 receptor messenger RNAs during embryonic development in the rat. *Neuroscience* **82**, 1131-1149.
- Chevalere V., Takahashi K.A. and Castillo P.E. (2006) Endocannabinoid-mediated synaptic plasticity in the CNS. *Annu. Rev. Neurosci.* **29**, 37-76.
- Clagett-Dame M., McNeill E.M. and Muley P.D. (2006) Role of all-trans retinoic acid in neurite outgrowth and axonal elongation. *J. Neurobiol.* **66**, 739-756.
- Dehmelt L., Smart F.M., Ozer R.S. and Halpain S. (2003) The role of microtubule-associated protein 2c in the reorganization of microtubules and lamellipodia during neurite initiation. *J. Neurosci.* **23**, 9479-9490.
- Digel M., Eehalt R. and Füllekrug J. (2010) Lipid droplets lighting up: insights from live microscopy. *FEBS Lett.* **584**, 2168-2175.
- Freund T.F., Katona I. and Piomelli D (2003) Role of endogenous cannabinoids in synaptic signaling. *Physiol. Rev.* **83**, 1017-1066.
- Galve-Roperh I., Aguado T., Rueda D., Velasco G. and Guzmán M. (2006) Endocannabinoids: a new family of lipid mediators involved in the regulation of neural cell development. *Curr. Pharm. Des.* **12**, 2319-2325.
- Gao Y., Vasilyev D.V., Goncalves M.B., Howell F.V., Hobbs C., Reisenberg M., Shen R., Zhang M.Y., Strassle B.W., Lu P., Mark L., Piesla M.J., Deng K., Kouranova E.V., Ring R.H., Whiteside G.T., Bates B., Walsh F.S., Williams G., Pangalos M.N., Samad T.A. and Doherty P. (2010) Loss of retrograde endocannabinoid signaling

and reduced adult neurogenesis in diacylglycerol lipase knock-out mice. *J. Neurosci.* **30**, 2017-2024.

Harkany T., Keimpema E., Barabás K. and Mulder J. (2008) Endocannabinoid functions controlling neuronal specification during brain development. *Mol. Cell. Endocrinol.* **286**, S84-90.

Harkany T., Guzmán M., Galve-Roperh I., Berghuis P., Devi L.A. and Mackie K. (2007) The emerging functions of endocannabinoid signaling during CNS development. *Trends Pharmacol. Sci.* **28**, 83-92.

He J.C., Gomes I., Nguyen T., Jayaram G., Ram P.T., Devi L.A. and Iyengar R. (2005) The G alpha(o/i)-coupled cannabinoid receptor-mediated neurite outgrowth involves Rap regulation of Src and Stat3. *J. Biol. Chem.* **280**, 33426-33434.

Hwang J.I., Kim H.S., Lee J.R., Kim E., Ryu S.H. and Suh P.G. (2005) The interaction of phospholipase C-beta3 with Shank2 regulates mGluR-mediated calcium signal. *J. Biol. Chem.* **280**, 12467-12473.

Jordan J.D., He J.C., Eungdamrong N.J., Gomes I., Ali W., Nguyen T., Bivona T.G., Philips M.R., Devi L.A. and Iyengar R. (2005) Cannabinoid receptor-induced neurite outgrowth is mediated by Rap1 activation through G(alpha)o/i-triggered proteasomal degradation of Rap1GAPII. *J. Biol. Chem.* **280**, 11413-11421.

Jung K.M., Astarita G., Zhu C., Wallace M., Mackie K. and Piomelli D. (2007) A key role for diacylglycerol lipase-alpha in metabotropic glutamate receptor-dependent endocannabinoid mobilization. *Mol. Pharmacol.* **72**, 612-621.

Jung K.M., Mangieri R., Stapleton C., Kim J., Fegley D., Wallace M., Mackie K. and Piomelli D. (2005) Stimulation of endocannabinoid formation in brain slice cultures through activation of group I metabotropic glutamate receptors. *Mol. Pharmacol.* **68**, 1196-1202.

Kano M., Ohno-Shosaku T., Hashimotodani Y., Uchigashima M. and Watanabe M.

- (2009) Endocannabinoid-mediated control of synaptic transmission. *Physiol. Rev.* **89**, 309-380.
- Katona I. and Freund T.F. (2008) Endocannabinoid signaling as a synaptic circuit breaker in neurological disease. *Nat. Med.* **14**, 923-930.
- Katona I., Urbán G.M., Wallace M., Ledent C., Jung K.M., Piomelli D., Mackie K. and Freund T.F. (2006) Molecular composition of the endocannabinoid system at glutamatergic synapses. *J. Neurosci.* **26**, 5628-5637.
- Mackie K. and Stella N. (2006) Cannabinoid receptors and endocannabinoids: evidence for new players. *AAPS J.* **8**, E298-306.
- Maejima T., Hashimoto K., Yoshida T., Aiba A. and Kano M. (2001) Presynaptic inhibition caused by retrograde signal from metabotropic glutamate to cannabinoid receptors. *Neuron* **31**, 463-475.
- Mátyás F., Urbán G.M., Watanabe M., Mackie K., Zimmer A., Freund T.F. and Katona I. (2008) Identification of the sites of 2-arachidonoylglycerol synthesis and action imply retrograde endocannabinoid signaling at both GABAergic and glutamatergic synapses in the ventral tegmental area. *Neuropharmacology* **54**, 95-107.
- Mulder J., Aguado T., Keimpema E., Barabás K., Ballester Rosado C.J., Nguyen L., Monory K., Marsicano G., Di Marzo V., Hurd Y.L., Guillemot F., Mackie K., Lutz B., Guzmán M., Lu H.C., Galve-Roperh I. and Harkany T. (2008) Endocannabinoid signaling controls pyramidal cell specification and long-range axon patterning. *Proc. Natl. Acad. Sci. USA* **105**, 8760-8765.
- Piomelli D. (2003) The molecular logic of endocannabinoid signalling. *Nat. Rev. Neurosci.* **4**, 873-884.
- Piomelli D. (2004) The endogenous cannabinoid system and the treatment of marijuana dependence. *Neuropharmacology* **47**, 359-367.
- Stella N., Schweitzer P. and Piomelli D. (1997) A second endogenous cannabinoid that



modulates long-term potentiation. *Nature* **388**, 773-778.

Tanimura A., Yamazaki M., Hashimotodani Y., Uchigashima M., Kawata S., Abe M., Kita Y., Hashimoto K., Shimizu T., Watanabe M., Sakimura K. and Kano M. (2010) The endocannabinoid 2-arachidonoylglycerol produced by diacylglycerol lipase  $\alpha$  mediates retrograde suppression of synaptic transmission. *Neuron* **65**, 320-327.

Uchigashima M., Narushima M., Fukaya M., Katona I., Kano M. and Watanabe M. (2007) Subcellular arrangement of molecules for 2-arachidonoyl-glycerol-mediated retrograde signaling and its physiological contribution to synaptic modulation in the striatum. *J. Neurosci.* **27**, 3663-3676.

Varma N., Carlson G.C., Ledent C. and Alger B.E. (2001) Metabotropic glutamate receptors drive the endocannabinoid system in hippocampus. *J. Neurosci.* **21**, RC188.

Walker D.J., Suetterlin P., Reisenberg M., Williams G. and Doherty P. (2010) Down-regulation of diacylglycerol lipase- $\alpha$  during neural stem cell differentiation: identification of elements that regulate transcription. *J. Neurosci. Res.* **88**, 735-745.

Watson S., Chambers D., Hobbs C., Doherty P. and Graham A. (2008) The endocannabinoid receptor, CB1, is required for normal axonal growth and fasciculation. *Mol. Cell. Neurosci.* **38**, 89-97.

Williams E.J., Walsh F.S. and Doherty P. (2003) The FGF receptor uses the endocannabinoid signaling system to couple to an axonal growth response. *J. Cell Biol.* **160**, 481-486.

Wu G., Lu Z.H. and Ledeen R.W. (1995) Induced and spontaneous neuritogenesis are associated with enhanced expression of ganglioside GM1 in the nuclear membrane. *J. Neurosci.* **15**, 3739-3746.

Yoshida T., Fukaya M., Uchigashima M., Miura E., Kamiya H., Kano M. and Watanabe M. (2006) Localization of diacylglycerol lipase- $\alpha$  around postsynaptic spine

**MOL#70458**

suggests close proximity between production site of an endocannabinoid, 2-arachidonoyl-glycerol, and presynaptic cannabinoid CB1 receptor. *J. Neurosci.* **26**, 4740-51.

## **Footnotes**

This work was supported by grants from the National Institute on Drug Abuse [ARRA R01 DA-012447].

## Legends for Figures

Figure 1. RA treatment induces differentiation of Neuro-2a cells, which is associated with increases in cellular 2-AG. Neuro-2a cells were incubated with 20  $\mu$ M *all-trans*-retinoic acid (RA) or vehicle (Veh). Morphological differentiation of the cells was noticeable starting from 24 hours of RA treatment (A). Neuro-2a cells were incubated with RA (20  $\mu$ M), DHPG (100  $\mu$ M) or carbachol (10  $\mu$ M) for 24 or 48 hours at 37°C. Cells were fixed, immunostained using anti- $\beta$ -Tubulin, and subjected to neurite outgrowth assays. Cellular processes which are at least two-fold longer than the corresponding cell body was regarded as neurites (n=6) (B). Neuro-2a cells were pre-treated with either vehicle or rimonabant (1  $\mu$ M, Rim) for 10 min and then added with 20  $\mu$ M RA for 24 hours (n=3) (C). Levels of cellular 2-AG and anandamide (D) and *in vitro* DGL activity (E) were measured at 48 hours of RA treatment (n=4). \*P< 0.05, \*\*P< 0.01, \*\*\*P< 0.001 by two-tailed *t*-test.

Figure 2. Functional expressions of both DGL- $\alpha$  and DGL- $\beta$  are required for RA induced differentiation of Neuro-2a cells. Neuro-2a cells were incubated with 20  $\mu$ M RA for the indicated times and DGL- $\alpha$  (A) or DGL- $\beta$  (B) mRNA levels were measured by quantitative real-time PCR. mRNA levels for CB<sub>1</sub> receptor (CB<sub>1</sub>R), MGL, ABHD6 and an internal control 18S were quantified after 3 days of RA treatment (n=4) (C). Neuro-2a cells were transfected with the following shRNA-expressing constructs; the non-targeting control (LacZi), DGL- $\alpha$ -targeting (DGL- $\alpha$ i), DGL- $\beta$ -targeting (DGL- $\beta$ i) or both DGL- $\alpha$ -targeting and DGL- $\beta$ -targeting (DGL- $\alpha$ i+DGL- $\beta$ i). After 24 hours, cells were treated with 20  $\mu$ M RA for 40 hours at 37°C (n=6) (D). Neuritogenic effects of 2-AG ether (Noladin ether, 10  $\mu$ M), a MGL inhibitor JZL184 (JZL, 1  $\mu$ M) and a ABHD6 inhibitor WWL70

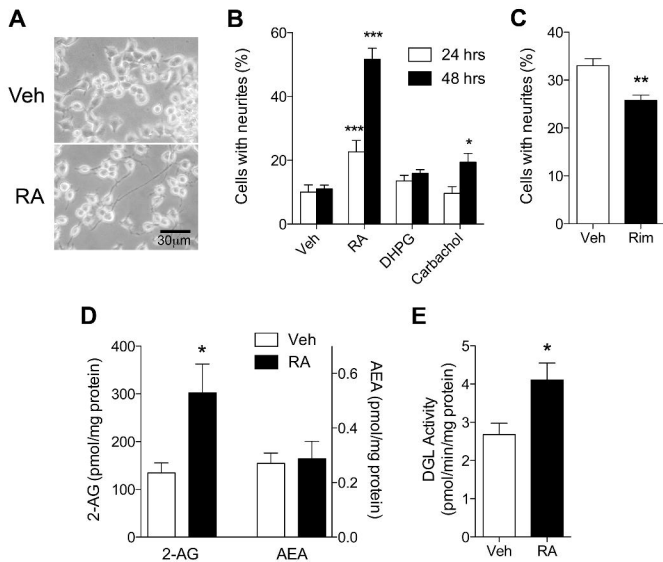
(WWL, 10  $\mu$ M) were determined upon 48 hours of treatments (n=6) (E). \*P< 0.05, \*\*P< 0.01, \*\*\*P< 0.001 by two-tailed *t*-test.

Figure 3. Recombinant DGL- $\beta$ -GFP protein localizes to lipid droplets in transfected cells. 48 hours after transfection of control pEGFP or DGL- $\beta$ -pEGFP vector in Neuro-2a cells (A) or HEK293 cells (B), cells were fixed and the nuclei were stained with DAPI (blue). Representative images under a fluorescence microscope are shown. V5-fused DGL proteins were expressed in Neuro-2a cells and visualized with anti-V5 antibody using Alexa 546 (red, Anti-V5) fluorescence. Co-stained in the cells were lipid droplets, using a fluorescent dye (green, BODIPY) which binds to neutral lipid. Arrows and arrowheads indicate lipid droplets and its co-localization with DGL- $\beta$ , respectively (C). After 24 hours from transfection with control pEGFP, DGL- $\alpha$ -pEGFP or DGL- $\beta$ -pEGFP vector, Neuro-2a cells were treated with 20  $\mu$ M RA for 40 hours at 37°C. Cells were fixed and stained with anti- $\beta$ -Tubulin antibody using Alexa 546 (red, Anti-Tubulin) fluorescence and DAPI (blue). Arrows indicate neurite localization of DGL- $\alpha$ -GFP or DGL- $\beta$ -GFP, whereas arrowheads indicate plasma membrane or lipid droplets distribution of DGL- $\alpha$  or DGL- $\beta$ , respectively (D).

Figure 4. Overexpression of DGL isoforms induces morphological changes in Neuro-2a cells. (A) Neuro-2a cells were transfected with control pEF6 (Vector), DGL- $\alpha$ -V5-pEF6 (DGL- $\alpha$ ) or DGL- $\beta$ -V5-pEF6 (DGL- $\beta$ ). After 72 hours of transfection, cells were fixed and double-immunostained with a rabbit polyclonal anti-V5 (for DGL staining) and a mouse monoclonal anti- $\beta$ -Tubulin (for  $\beta$ -Tubulin staining) antibodies. For DGL- $\alpha$  or DGL- $\beta$ , V5-positive cells were selected and the number of cells bearing neurite-like cellular processes were counted. (B) Representative images under a light microscope (top) or a

fluorescence microscope (bottom) of stable transfectants of pEF6 vector (P7), DGL- $\beta$ -V5 ( $\beta$ 14) or DGL- $\alpha$ -V5 ( $\alpha$ 18). Cells were immunostained using anti- $\beta$ -Tubulin antibody (green fluorescence) and the nuclei were stained with DAPI (blue). Percentage of cells containing neurite processes (C) and mean lengths of the neurites (D) were measured from the P7,  $\alpha$ 18 or  $\beta$ 14 stable cell lines. \* $P$  < 0.05, \*\* $P$  < 0.01, \*\*\* $P$  < 0.001 by two-tailed  $t$ -test.

Figure 5. Antagonism of CB<sub>1</sub> receptor selectively blocks neurite outgrowth induced by DGL- $\alpha$  expression. The stable DGL-expressing Neuro-2a cells  $\alpha$ 18 and  $\beta$ 14, along with the control P7 cells, were treated for 24 hours with 1  $\mu$ M rimonabant (Rim), a CB<sub>1</sub> receptor antagonist, in serum-free media. Cells were then fixed, immunostained using anti- $\beta$ -Tubulin, and subjected to neurite outgrowth assays. \*\*\* $P$  < 0.001 by two-tailed  $t$ -test.



**Fig. 1**

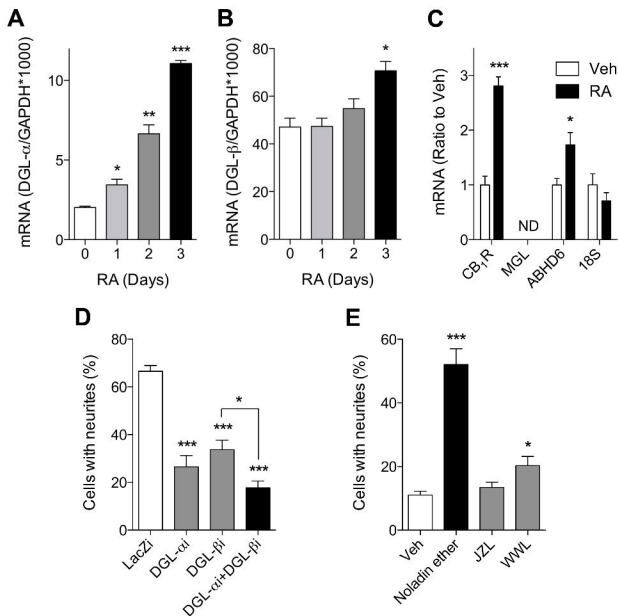


**Fig. 2**



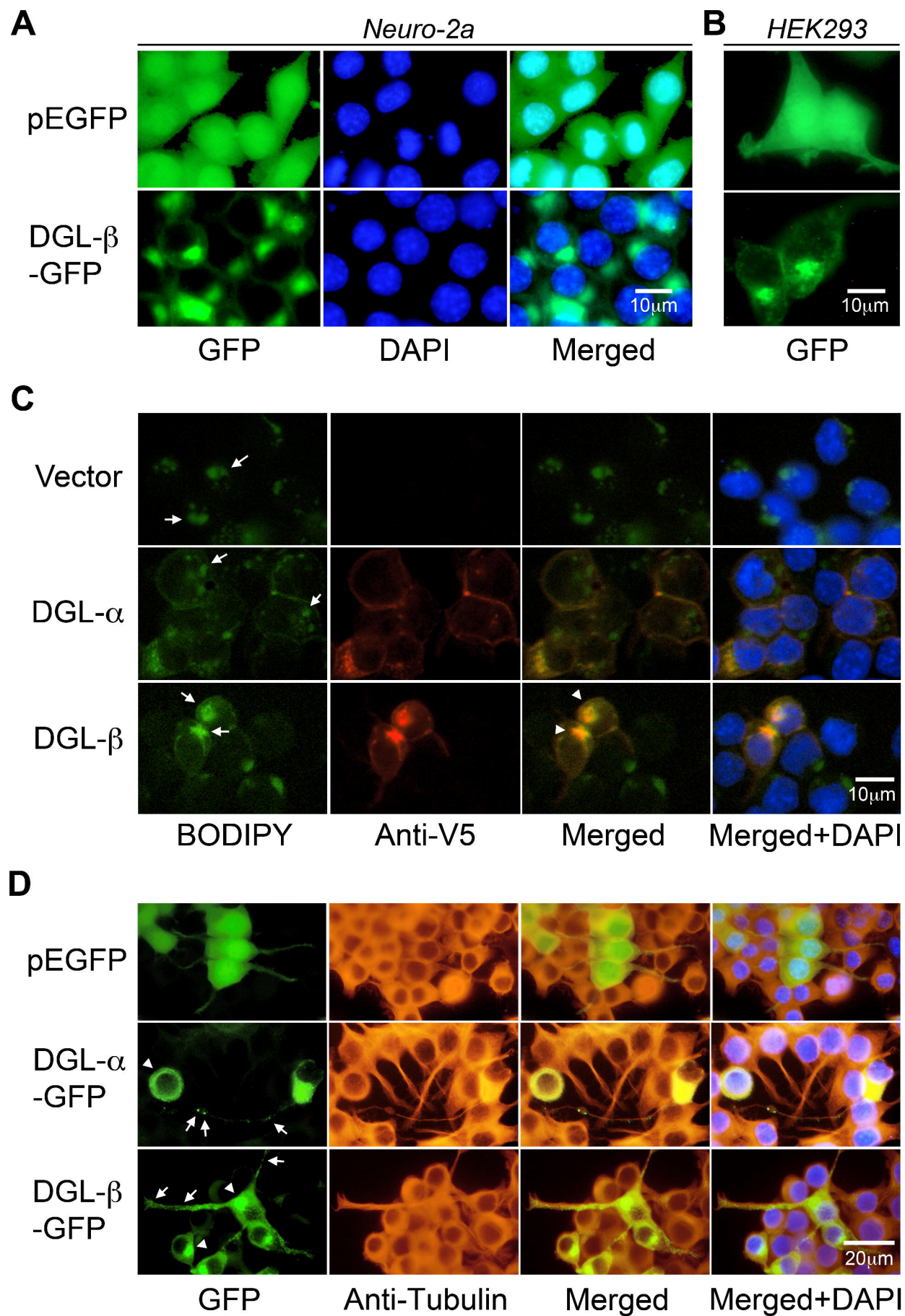


**Fig. 3**

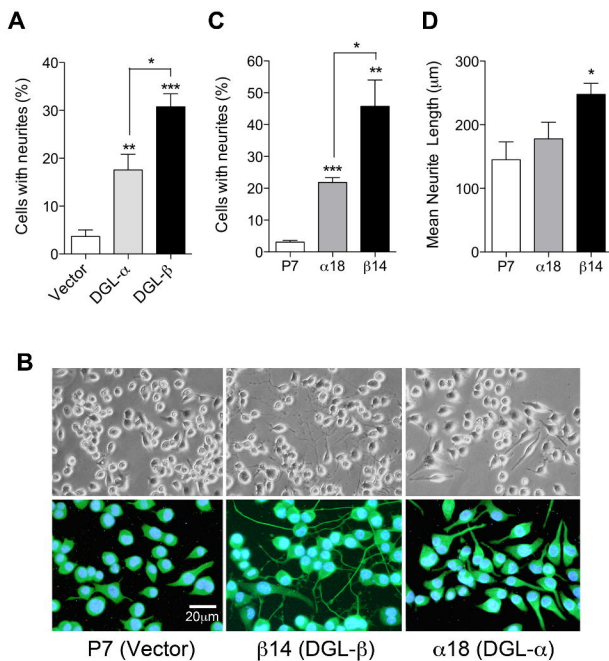


**Fig. 4**

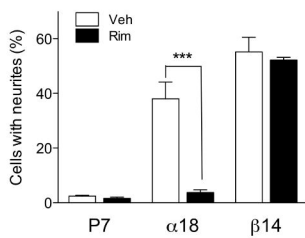


**Fig. 5**

## **Supplementary Data**

Diacylglycerol lipase- $\alpha$  and - $\beta$  control neurite outgrowth in Neuro-2a cells through distinct molecular mechanisms. Jung, K.-M, Astarita, G., Thongkham, D. and Piomelli, D. Molecular Pharmacology.

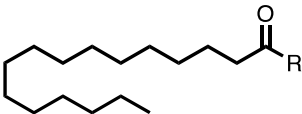
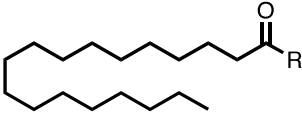
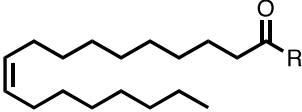
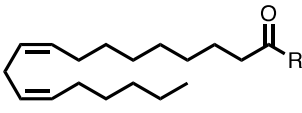
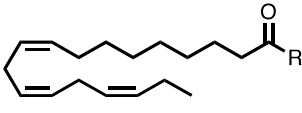
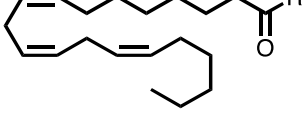
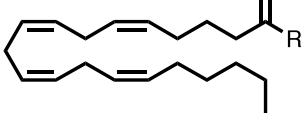
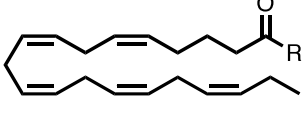
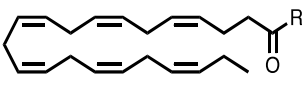
Supplementary Table 1

Supplementary Figure S1

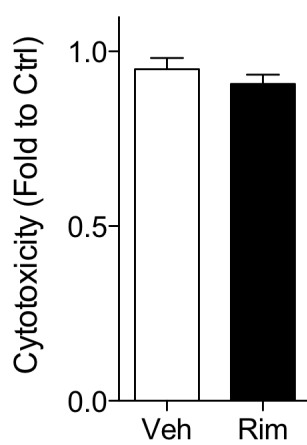
Supplementary Figure S2

Supplementary Figure Legends

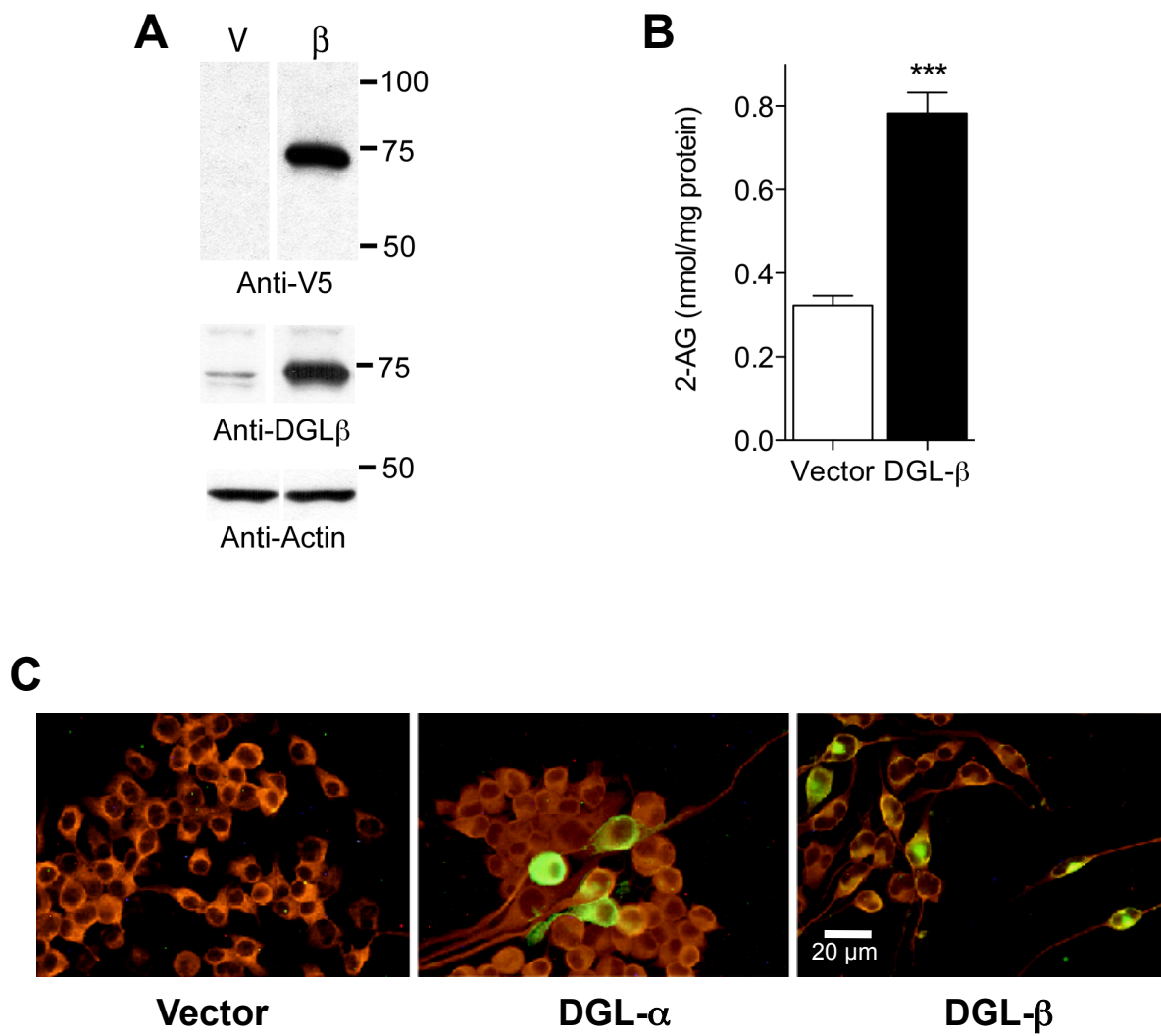
Supplementary Table I. MAG (R=glycerol) and FA (R=OH) levels (pmol/mg protein) in Neuro-2a cells following DGL- $\beta$  overexpression (n=4).

Acyl Chain	Structure	Lipid	m/z	Vector	DGL- $\beta$
16:0		MAG	353	278 $\pm$ 8	278 $\pm$ 10
		FA	255	293 $\pm$ 7	309 $\pm$ 7
18:0		MAG	381	51 $\pm$ 9	41 $\pm$ 2
		FA	283	414 $\pm$ 19	448 $\pm$ 27
18:1 $\Delta^9$		MAG	379	206 $\pm$ 18	259 $\pm$ 11
		FA	281	158 $\pm$ 1	181 $\pm$ 5**
18:2 $\Delta^{9,12}$		MAG	377	29 $\pm$ 3	50 $\pm$ 4*
		FA	279	10 $\pm$ 1	11 $\pm$ 0.6
18:3 $\Delta^{9,12,15}$		MAG	375	9 $\pm$ 2	21 $\pm$ 7
		FA	277	0.8 $\pm$ 0.1	0.5 $\pm$ 0.1
20:3 $\Delta^{8,11,14}$		MAG	403	59 $\pm$ 7	95 $\pm$ 4**
		FA	305	3.5 $\pm$ 0.1	4.0 $\pm$ 0.1*
20:4 $\Delta^{5,8,11,14}$		MAG	401	322 $\pm$ 23	782 $\pm$ 49***
		FA	303	11 $\pm$ 0.5	15 $\pm$ 0.6**
20:5 $\Delta^{5,8,11,14,17}$		MAG	399	12 $\pm$ 1	22 $\pm$ 5
		FA	301	3.7 $\pm$ 0.4	4.8 $\pm$ 0.6
22:6 $\Delta^{4,7,10,13,16,19}$		MAG	425	9.6 $\pm$ 0.5	20 $\pm$ 1***
		FA	327	0.5 $\pm$ 0.0	0.4 $\pm$ 0.1

Values are means  $\pm$  SEM, n=3-4. \*\*\* $P$ <0.001, \*\* $P$ <0.01, \* $P$ <0.05 by two-tailed Student's  $t$ -test.



**Supplementary Fig. S1**



**Supplementary Fig. S2**

### Legends for Supplementary Figure

Supplementary Figure S1. Exposure to rimonabant does not cause cytotoxicity in Neuro-2a cells. Neuro-2a cells were pre-treated with either vehicle (DMSO, Veh) or rimonabant (1  $\mu$ M, Rim) for 10 min and then added with 20  $\mu$ M RA for 24 hours at 37°C. Levels of lactate dehydrogenase (LDH) released into the cultured media were measured using cytotoxicity detection kit, LDH (Roche, Indianapolis, IN) and the values were normalized by no treatment control (n=8).

Supplementary Figure S2. Overexpression of DGL isoforms induces morphological changes of Neuro-2a cells. (A) Neuro-2a cells were transfected with control pEF6 vector (V) or DGL- $\beta$ -V5-pEF6 ( $\beta$ ). Cells were harvested 72 hours after transfection and the expression of DGL- $\beta$ -V5 protein was assessed by western blot analyses using anti-V5 (top) or anti-DGL- $\beta$  (middle) antibody (Jung *et al.*, 2007). Both antibodies recognized a band of approximately 70 kDa, which was highly expressed in DGL- $\beta$  transfected cells. Actin (bottom) serves as a loading control. (B) The levels of 2-AG were determined under the same condition by a LC-MS method (n=4). (C) Neuro-2a cells were transfected with control pEF6 (Vector), DGL- $\alpha$ -V5-pEF6 (DGL- $\alpha$ ) or DGL- $\beta$ -V5-pEF6 (DGL- $\beta$ ). After 72 hours of transfection, cells were fixed and double-immunostained with a rabbit polyclonal anti-V5 (for DGL staining, green) and a mouse monoclonal anti- $\beta$ -Tubulin (for  $\beta$ -Tubulin staining, red). Representative fluorescence microscope images were shown. \*\*\* $P$ <0.001 by two-tailed  $t$ -test.